ChemElectroChem

Research Article
doi.org/10.1002/celc.202300517

Chemistry Europe
European Chemical Societies Publishing

www.chemelectrochem.org

Understanding the Role of Additives on The Electrochemistry and Performance of Zn Energy Storage Devices

L. N. Bengoa,*[a] R. M. González-Gil,[a] and P. Gómez-Romero*[a, b]

As the interest in alternative Li-based energy storage technologies increased during the last years, zinc emerged as a promising candidate. Despite several advantages over Li, Zn cycling stability is still a major issue. In this article, the use of near-neutral electrolytes (non-expensive 2 M $ZnSO_4$) with the addition of different additives (dimethylsulfoxide and tetratethylammonium chloride) is proposed as a solution. The Zn deposition/dissolution electrochemistry has been evaluated and the cycling stability was determined in Zn//Zn symmetric coin-cells. Hybrid supercapacitors were also assembled and tested in a range of 0.2 V–1.8 V for 2000 cycles, using activated carbon electrodes as cathode and Zn foil as anode. The results show that dimethylsulfoxide strongly inhibits the Zn deposition process, evidenced by a decrease in the cathodic current density, as well as in the dissolution peak. DMSO affects the deposition mechanism, whereas tetratethylammonium chloride reduces the exchange current density, consistent with the adsorption of tetraethylammonium ions on the Zn surface. A synergy between both additives leading to further inhibition of Zn^{2+} reduction is observed allowing cycling up to 250 hours for Zn//Zn devices. In addition, the performance of hybrid supercapacitors has also improved showing better capacity and extended cycle life.

Introduction

Over a decade has passed since governments around the world and the society in general have become aware that an in-depth modification of our production system is needed to stop and, ideally, mitigate climate change.[1] However, both the proper integration of intermittent (renewable) energy sources into electricity grids and the widespread adoption of EVs largely rely on the use of efficient electrically rechargeable energy storage devices. For several years, Li-ion batteries (LIBs) have dominated the market due to their relatively high energy density, acceptable power density, and good cycle life,[2] becoming the leading technology when it comes to portable electronics and current EVs. However, the intercalation chemistry in LIBs limits their energy density ($<350\ Wh\,kg^{-1}$) making them unsuitable for large scale applications or long range EVs.[3,4] There are also several concerns regarding their high cost and inherent safety hazards.[5] On top of this, the scarcity of raw materials (such as Li and cathode components) and questionable mining practices taking place in third world countries, together with the expected increase in demand from the battery sector, indicate that LIBs are currently not a sustainable option.[6] All these issues have triggered the search for alternative energy storage technologies that can not only provide the required performance but also be produced in a sustainable way, i.e. without comprising the needs of future generations.

Many post-Li chemistries have been proposed, among which aqueous metal batteries have attracted a lot of attention since they avoid the use of typically flammable, unsafe, and toxic organic solvents. Furthermore, significant cost reductions can be achieved since device assembly can be done under atmospheric conditions.[7] Alkali and multivalent metal-ion aqueous batteries have been designed,[8] but Zn-based energy storage devices are currently the most attractive ones.[9] Metallic zinc can be directly used as an anode due to low redox potential which makes it stable in water and air. Moreover, this is a low-cost[10] material which also presents both high theoretical specific and volumetric capacities ($820\ mAh\,g^{-1}$ and $5854\ mAh\,cm^{-3}$). In terms of sustainability, Zn is 300 times more abundant than Li[12] and can be easily recycled[13], which could boost the development of a circular battery economy. All these features make rechargeable Zn-based devices promising and attractive candidates to take over the market of next-generation energy storage technologies. Despite all the positive properties and regardless of the cathode chemistry (e.g. Zn-ion,[9,11,12] Zn-air,[1,13,14] Zn-hybrid[15–17]), they suffer from severe anode degradation upon cycling, which has prevented it widespread commercialization. Several factors affect the performance of Zn as anode, which include H_2 evolution (causing self-discharge), surface passivation and shape changes and/or dendritic growth

[a] Dr. L. N. Bengoa, Dr. R. M. González-Gil, Prof. Dr. P. Gómez-Romero
Catalan Institute of Nanoscience and Nanotechnology (ICN2), CSIC and BIST,
Campus UAB, Bellaterra, 08193 Barcelona, Spain
E-mail: pedro.gomez@icn2.cat
leandro.bengoa@icn2.cat

[b] Prof. Dr. P. Gómez-Romero
Consejo Superior de Investigaciones Científicas (CSIC)

Supporting information for this article is available on the WWW under https://doi.org/10.1002/celc.202300517

due to non-uniform current distributions.[1,18] In an attempt to minimize these phenomena, near-neutral or mildly acidic electrolytes have been tested instead of the highly alkaline 6 M KOH, commonly used in non-rechargeable Zn-air batteries. At these mild conditions Zn/Zn^{2+} kinetics are more sluggish than at extreme pH values, which decreases the possibilities of dendrite formation, while Zn inhomogeneous dissolution is significantly reduced. This translates into improved cycle life and higher stability of Zn anodes.[19] Unfortunately, this is usually not enough to meet the demanding requirements of current and future applications and other actions need to be implemented.

The addition of organic compounds to the electrolyte to control the deposit quality and morphology has been used in the electroplating industry for almost a century,[20–23] and has already proved to be a successful approach to improve the cycle life of Zn anodes. These additives can be classified either as leveling agents, brighteners, or complexing agents[20], and usually a combination of two or more kinds of additives is needed. Leveling agents adsorb at high current density points, blocking them and favoring deposition on low current density spots. The working principle of brighteners is still under discussion, but it is mostly believed that they have specific interactions with certain crystallographic planes affecting the preferred crystal growth direction, which leads to smoother and brighter (in terms of light reflectance) coatings. Finally, complexing agents affect the reaction mechanism (equilibrium potential, overpotential and kinetics), due to the change in the chemistry of the main active species in the electrolyte. Synergies between additives have been largely reported both in electrodeposition[21,22] or battery[23,24] focused articles.

In recent years dimethylsulfoxide (DMSO), a low toxicity solvent,[25] has been tested as an additive in many types of Zn-based energy storage technologies, yielding important improvements in cycle life and stability. This organic solvent can act as a complexing agent, replacing water molecules from Zn^{2+} solvation sphere, and form strong bonds with H_2O reducing its activity towards reduction.[26,27] Both effects hinder dendrite formation thus increasing the cycling stability of Zn anodes. On the other hand, quaternary ammonium compounds (QAC) have been known to have a positive effect on the morphology of Zn deposits for decades and are now being considered in the formulation of electrolytes for Zn based devices.[28–30] These cationic surfactants adsorb on the surface of Zn forming a barrier that controls the reaction rate,[31–33] mitigating common issues of Zn anode such as dendritic growth and H_2 evolution. Even though there are several reports on the use of either DMSO or QAC as additives in neutral electrolytes, the combination of both types of organic substances has not been considered yet, which could bring about further improvements in Zn-devices cycle life.

Based on the lack of this kind of studies, the present work explores the synergic effect between DMSO (complexing agent) and tetratethylammonium chloride (TEACl) as QAC in the Zn deposition/dissolution processes and its subsequent impact on the cycling stability of Zn anodes. The experimental approach used involves both three and two-electrode cells (coin cells) measurements. The former provided valuable (qualitative and quantitative) information on the inhibitory effect of these additives on the electrochemistry of Zn. This was then correlated with the traditional, time-consuming, cycling experiments currently performed in the field of battery research. The results show that the combination of DMSO and a QAC can lead a considerable improvement in the cycling stability of Zn anodes in a $ZnSO_4$ electrolyte, which was validated in lab scale Zn-hybrid devices, using commercial activated carbon as capacitive cathodes. The proposed methodology is not only effective but serves as a starting point for future research considering that the list of QAC is vast and diverse.

Experimental section

This work was conducted using 2 M $ZnSO_4$ electrolyte to which either 20 wt.% DMSO, 0.25 M TEACl or both were added to assess the effect of these additives in the electrochemistry of Zn deposition and dissolution. The electrolytes were prepared by dissolution of the proper amounts of $ZnSO_4{\cdot}7\ H_2O$ (Sigma Aldrich, 99 wt.%) and TEACl (Sigma Aldrich, 98 wt.%) in either ultrapure water or a water/DMSO (Sigma Aldrich, 99.7 wt.%) mixture with a 4:1 mass ratio (20 wt.% of DMSO). All the chemicals were used as received. The electrolyte conductivity was measured by EIS applying a 5 mV perturbation at the E_{OCP} in the frequency range 10–100 kHz. These experiments were carried out in a homemade rectangular cell with two parallel stainless-steel electrodes and a cell constant of 0.4875 cm^{-1}.

Cyclic (CV) and linear sweep (LSV) voltammetry were recorded in a three-electrode cell configuration using a Pt wire and a Ag/AgCl (3.5 M NaCl, E_{ref} = 0.195 V vs SHE) electrode as counter and reference electrodes, respectively. For CV, measurements were performed on a glassy carbon electrode (d = 3 mm) at 50 $mV\,s^{-1}$ to do a qualitative characterization of the different formulations proposed. On the other hand, LSV were conducted on a high purity Zn electrode (99.97%, Goodfellow 100 μm foil), previously polished to remove any oxide film on the surface, at low scan rates (0.016 $mV\,s^{-1}$) typically used for Tafel plots acquisition, to determine Zn^{2+} reduction kinetic parameters. Galvanostatic deposition experiments were performed on 1 cm^2 Cu (99.95%. Goodfellow) substrates to evaluate the effect of additives on Zn morphology and microstructure. A two-electrode cell was used, and deposits were obtained at 0.5 $mA\,cm^{-2}$ up to a charge of 2 $mAh\,cm^{-2}$ (~3 μm thickness). Prior to deposition, Cu substrates were first cleaned with ethanol, then pickled in 1:10 HCl (37%) dilution for 30 s. After this, substrates were rinsed with water and immediately immersed in the plating solution. The morphology of the obtained deposits was characterized by SEM using a Quanta 650 FEG microscope equipped with EDS Inca X-Max 20 detector (Oxford instruments). XRD patterns were acquired using a Malvern Panalytical X'pert Pro Materials Powder Diffractometer with CuKα radiation (λ = 1.54 Å) and a nickel filter. The detector was swept between 5° – 80° with a step size of 0.05° and 3.5 s per step.

Zn platting/stripping Coulombic efficiency (CE) was determined in a 2-electrode coin cell (CR2032) configuration using Cu (pretreated as described before) as substrate and Zn foil as counter electrode. Deposition and dissolution were carried out for 50 cycles at 0.5 and 2 $mA\,cm^{-2}$. For this experiment, a charge of 0.5 $mAh\,cm^{-2}$ was set for the deposition period, while a cut-off voltage of 0.8 V was used as a limit in the dissolution step. Cycling stability of Zn in the different electrolytes was assessed using Zn//Zn symmetric CR2032 cells, which were cycled at 0.5 $mA\,cm^{-2}$ and 0.5 $mAh\,cm^{-2}$ until

failure was detected. These values were selected to match those traditionally used in ZIB literature. However, it should be noted that this depth of discharge is lower than those for practical battery operation.[34] Finally, hybrid Zn//Activated carbon (AC) supercapacitor devices were assembled to test the electrolytes in operating devices. AC electrodes (Kurakay YP-80F) were prepared by slurry casting, after mixing this material with PVDF at a weight ratio of 90:10. The solid mixture was then dispersed in 1-methyl-2-pyrrolidone solvent, coated on top of 10 μm stainless steel foil and vacuum dried at 100 °C overnight. The AC electrodes were then cut (10 mm) and characterized by CV in a 3 electrode Swagelok cell using heavily AC loaded carbon cloth and Ag/AgCl as counter and reference electrodes, respectively. For coin-cell configuration (CR2032) tests, electrodes were cut to 14 mm and glass fiber (Whatmann 1825, 0.42 mm thick) was used as separator. They were cycled at 0.5 A g^{-1} (based on the cathode active material) in the range 0.2 V–1.8 V for 2000 cycles. To evaluate the effect of cycling on the Zn morphology and microstructure, anodes were removed from the cells and characterized by SEM and XRD.

Results and Discussion

The CVs of the different electrolytes tested in this work are shown in Figure 1 and Figure S1. Regardless of the composition, the curves present a typical shape for Zn deposition/dissolution generally observed in acid electrolytes.[35] A single reduction process is detected in the cathodic branch corresponding to the two-electron reduction of Zn^{2+}[36] and just one dissolution peak appears during the anodic scan. The latter suggests that no oxides/hydroxides form on the surface of Zn during oxidation as opposed to what has been reported for alkaline electrolytes.[37,38] The addition of DMSO, TEACl or both clearly inhibits the electrochemical process reducing the cathodic current density, which translates into a decrease of the anodic peak area. However, the results also show that DMSO inhibitory effect is more significant than that of TEACl, and that there is a synergy between both additives leading to a further decrease of current density. While both substances have a similar impact on the CV, some features already suggest that they alter Zn electrochemistry through different mechanisms. First, the slope of the cathodic branch is lower when DMSO is present in the electrolyte formulation, while it remains virtually unchanged when TEACl is added (no DMSO). Furthermore, the anodic peak's potential shifts towards higher E values only after addition of DMSO. The change in the slope caused by the latter on the cathodic part of the CV, is likely related to its complexing ability of Zn^{2+} ions as has been previously reported for other aqueous.[26,27,39] On the other hand, the peak's potential is usually linked to the composition and microstructure of the dissolving phase.[40] Therefore, DMSO might be either inducing the formation of a secondary phase or affecting the preferential growth direction of the deposit. The inset in Figure 1 shows that the Zn discharge potential at which the reduction starts, moves in the cathodic direction in the electrolytes containing additives. This further confirms the DMSO-Zn^{2+} interactions. As regards TEACl, it is known that QAC cations can adsorb on the surface of either Zn or the glassy carbon electrode, limiting the reaction rate and polarizing the deposition process.[32,33] The coulombic efficiency estimated from the CVs (Table 1), indicates that both additives also inhibit H_2 evolution to some extent.

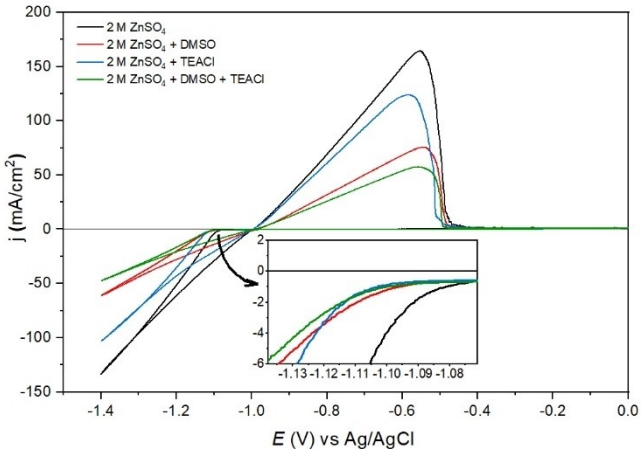

Figure 1. CVs recorded at 50 mV s^{-1} on a still glassy carbon electrode

The qualitative analysis done with the data from CV was further confirmed by determination of the reduction kinetic parameters (Table 1) from slow scan rates LSV (Figure 2). The results support the effect of both additives described in the previous paragraphs. DMSO changes the cathodic charge transfer coefficient α_c from ≈1.5 to values close to 1. Since Zn^{2+} reduction takes place through a multistep (electrochemical and chemical) reaction mechanism,[41–43] the variation of α_c could be due to either changes in the symmetry factor (β) or the rate determining step (see Eq. 1).[44,45] In contrast, TEACl has no significant impact on the Tafel slope value, but greatly reduces the exchange current density (j_0) as a result of the adsorption of this additive on the surface of Zn. The results also confirm the interaction between both additives, showing that in a DMSO containing electrolyte, the reduction in j_0 caused by TEACl is somewhat smaller. However, based on the CV in Figure 1, it can

Table 1. Electrolyte conductivity and Zn kinetic parameters determined from Tafel plots in Figure 2.

Electrolyte	σ (mS cm^{-1})	Q_{an}/Q_{Cat}*100[a]	E_{OCP} (V)	b_C (mV dec^{-1})	α_C	$j_0 \times 10^1$ (mA cm^{-2})
2 M ZnSO4	52.16	95	−0.985	38.43	1.54	8.91
2 M ZnSO4 + DMSO	22.70	98	−0.986	65.79	0.90	2.62
2 M ZnSO4 + TEACl	49.95	98	−0.989	41.27	1.43	1.19
2 M ZnSO4 + DMSO + TEACl	20.14	98	−0.983	55.43	1.07	2.09

[a] Current efficiency calculated from CV in Figure 1.

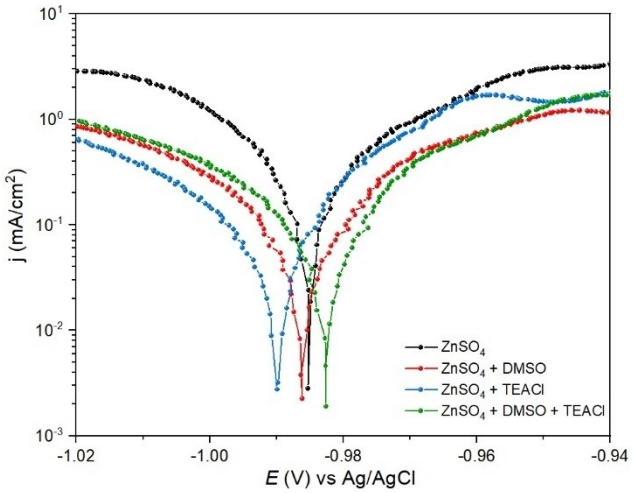

Figure 2. Tafel plots for different electrolytes measured at 0.016 mV s^{-1} on a Zn electrode.

be concluded that overall the combination of DMSO and TEACl limits and controls the Zn deposition rate through both a change in the reduction mechanism and an electrode-blocking adsorption.

$$\alpha_c = n_p + n_{rds}\beta \quad (1)$$

One final and comment on the effect of additives is related to the decrease in the specific conductivity cause by DMSO. While this is not unexpected it should be taken into account on the design of energy storage devices.

The morphology of Zn deposits obtained in the different electrolytes is shown in Figure 3 and Figure S2. In the absence of additives (Figure 3-a), a mossy (or sponge-like) deposit develops, typical of Zn deposition at low overpotentials. This morphology is usually observed for metals that fall within Winand's 'normal' definition,[46] due to their large j_0 values which lead to diffusion or mixed control deposition without the need of applying large overpotentials.[47,48] It is worth noting that apart from these rounded clusters, there are large Zn hexagonal crystals in the flat surface of the coating. At these spots, current density would be lower than at the upper part of the mossy structures, therefore allowing for an activation-controlled deposition. However, most of these platelets are facing upwards and thus can act as dendrite initiators.[49] The change in the electrochemistry induced by DMSO (Figure 3-b), reflects on the morphology of the deposits. The reduction in j_0 translates into a refinement of the Zn grains (flat part of the electrode), which could retard the formation of dendrites upon cycling. Nevertheless, high current density points are not avoided, and spongy deposits still develop, but their size is considerably smaller. On the other hand, TEACl (Figure 3-c) has a strong leveling and grain refinement effect, as expected in the case of adsorbing organic additives.[50] When both compounds are present in the solution (Figure 3-d), a relatively flat morphology is obtained, known as ridge[51], in which Zn crystals are tilted with their pyramidal planes pointing up. A larger grain size is observed when compared to the solution only containing TEACl. This again suggests that there is an interaction between both substances as previously inferred from electrochemical data.

The XRD patterns displayed in Figure 4 show that in all cases metallic Zn (JCPDS-ICDD 00-004-0831) is the only deposited phase, without the presence of sulfur containing compounds present in the surface, except for the additive free electrolyte which shows a small amount of hydrated $ZnSO_4$ precipitate. Considering the highly porous structure of this film, this probably arises from dried electrolyte that could not be removed during the washing step. Copper substrate diffraction peaks are also visible in the pattern together with some other which can be assigned to a $CuZn_5$ intermetallic phase,[28] which can form during the initial stages of deposition due to the

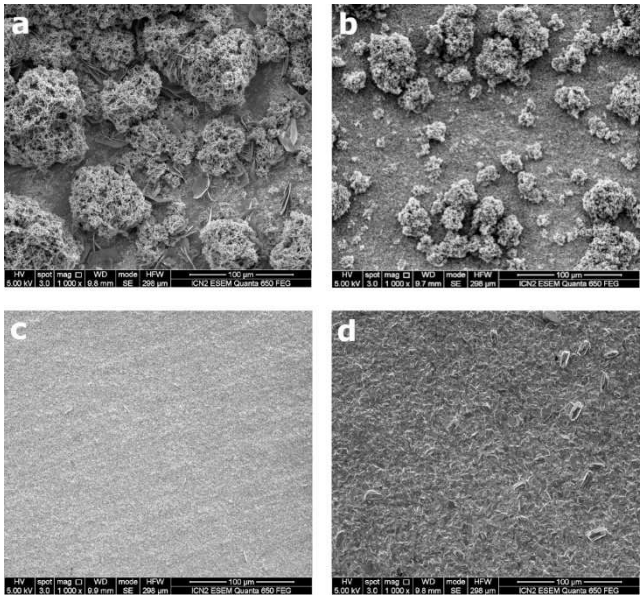

Figure 3. SEM images of Zn deposits obtained on Cu substrates at 0.5 mA/cm² in different electrolytes: (a) 2 M $ZnSO_4$, (b) 2 M $ZnSO_4$ + DMSO (20 wt.%), (c) 2 M $ZnSO_4$ + 0.25 M TEACl and (d) 2 M $ZnSO_4$ + DMSO (20 wt.%) + 0.25 M TEACl.

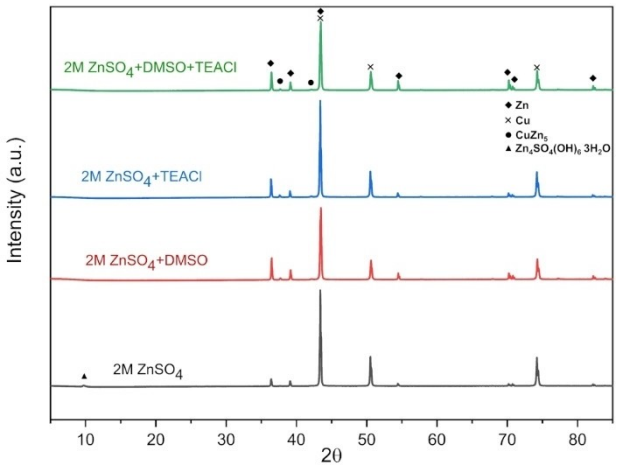

Figure 4. XRD patterns of Zn deposits.

underpotential deposition (UPD) and insertion of Zn into the Cu lattice.[52,53]

The effect of additives on the CE for Zn plating/stripping was studied in Cu//Zn coin cells for 2 different current densities. Figures 5-a and 5-b show the evolution of this parameter with the cycle number, showing that after an initial period, the CE reaches a stable value between 95–98% for all the experimental conditions. Such a behavior has been reported before,[27] and could be related to an alloying effect.[54] Based on XRD results, the lower values during the first cycles may stem from the formation of $CuZn_5$ phase that is not dissolved in the anodic step. Being a different phase than pure Zn, its dissolution potential could be higher and hence the 1 V limit set for the experiment might not be high enough. However, after a few cycles, the Cu lattice would saturate of Zn and further formation of this intermetallic might be strongly inhibited, leading to a higher and stable CE. The latter could also explain the higher CE observed at higher current densities. Zn diffusion into the Cu matrix is likely a slow process that happens when UPD leads to the formation of a monolayer (complete or partial). Under these conditions, the metal-substrate interaction dominates, and diffusion of Cu–Zn alloying can occur.[55,56] However, at

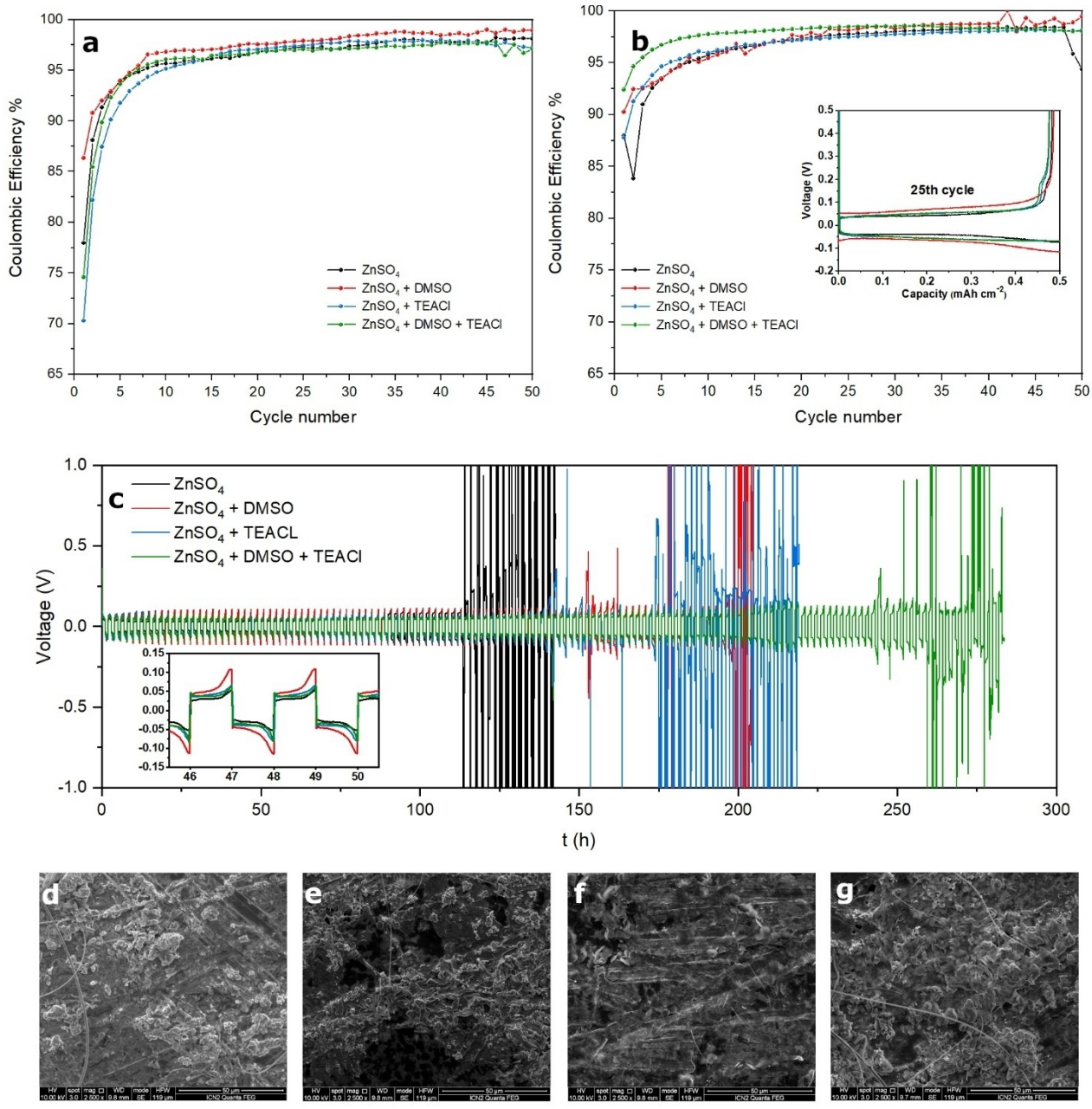

Figure 5. Zn plating/stripping coulombic efficiency determined in Cu//Zn coin-cells at (a) 0.5 mA cm^{-2} and (b) 2 mA cm^{-2} for a total charge of 0.5 mAh cm^{-2}. (c) Cycling stability tests of Zn//Zn symmetrical cells at 0.5 mA cm^{-2} and 0.5 mAh cm^{-2}. The inset shows the deposition/dissolution profiles for all electrolytes. SEM images of Zn electrode after 20 cycles in Zn//Zn symmetric cells (electrode shown was subjected to a deposition step during the last cycle): (a) 2 M $ZnSO_4$, (b) 2 M $ZnSO_4$ + DMSO (20 wt.%), (c) 2 M $ZnSO_4$ + 0.25 M TEACl and (d) 2 M $ZnSO_4$ + DMSO (20 wt.%) + 0.25 M TEACl.

higher current densities Zn islands will form at a higher rate providing a stronger metal-metal interaction that might limit the penetration of Zn into the Cu lattice. In addition to this, another factor affecting the CE is H_2 evolution, a common side reaction at deposition conditions. The way in which this parasitic reaction affects the CE values is complex since H_2 kinetics are strongly dependent on the surface composition. Therefore, the amount of H_2 will be different during the first cycles when deposition takes place on "pure" copper, than after the previously described alloying process. The latter will affect the kinetical parameters of H^+ reduction. Moreover, once a complete layer of Zn forms on top of the substrate, these parameters will change again. Regardless of these different stages in the deposition step, H_2 can not be neglected and will have a negative impact on the plating/stripping efficiency. The incremental loss of Zn mass for these experiments is represented in Figures S3 a and b. This parameter represents the excess of Zn that would be necessary to place in a battery to compensate the loss of material due to coulombic efficiency issues.[57] The results show that even though the CE reaches a similar stable value for all the electrolytes, the lower initial values mean that a higher excess of Zn is needed to achieve good cycle life of Zn devices.

However, it should be noted that no significant differences between electrolytes can be seen in terms of CE, in agreement with data estimated from the CVs in Fig.1. On the other hand, the addition of either DMSO or TEACl extends the cycle life of a Zn//Zn symmetrical cell (Figure 5-c), suggesting that the inhibition effect observed in electrochemical data and the morphology changes, translate into higher cycling stability. Similar improvements have been reported after the addition of DMSO by different authors, who have ascribed this effect to the modification of the solvation sheath (hindering side reactions) and the changes in the preferred crystal orientation (smooth deposits with a 002 texture) .[26,27] Likewise, several studies have demonstrated the beneficial effect of some QAC, with TBA showing the best results so far.[28,29] The mechanism through which these cationic substances affect the electrochemical process is clear and related to the adsorption on the surface of the electrode, creating a barrier that controls the reaction rate. An exhaustive study of QAC with different chemical structure was conducted by Bozzini et al.,[29] showing that inhibition of the cathodic reaction is the main factor leading to the improvement in cycling stability. The synergetic effect between a complexing agent as DMSO together with an adsorbing additive, allows cycling for almost 250 h in comparison with the 120 h achieved in the absence of additives. The further improvement in Zn stability obtained with both additives may be ascribed to the stronger inhibitory effect evidenced in the CV. The inset in Figure 5-c also shows that after some cycles the overvoltage for the electrolyte containing only DMSO is the highest one, which may be a consequence of the formation of a passivation layer. It is also interesting to note that in all the electrolytes, the failure occurs through a passivation mechanism and no short-circuiting is detected.[29] The morphology of Zn electrodes after 20 cycles in Zn//Zn symmetrical cells is shown in Figs. 5 d-g and Figure S4. The effect of additives described before (Fig.3 deposition experiments), can also be observed in these SEM images. In a 2 M $ZnSO_4$ electrolyte, large Zn islands grow perpendicular to the surface. At higher magnifications (Figure S4) the presence of hexagonal platelets randomly oriented can be detected in agreement with previous reports.[58] Addition of DMSO leads to a rather smoother deposit, with Zn crystals exposing the pyramidal planes towards the electrolyte. However, isolated protruding deposits can be observed along the electrode surface (Figure S4-c), which correlates with results from deposition experiments (Figure 3 and Figure S2-b), where an improvement in Zn morphology was detected but spongy-like areas are still present. Likewise, after cycling, TEACl yields the best surface morphology with some large Zn hexagonal platelets parallel to the surface. When both DMSO and TEACl are present in the electrolyte, the morphology is mostly similar to that obtained when only DMSO was added. Nevertheless, in this case no large Zn protuberances form, which could explain the better cycling stability in the $ZnSO_4 + DMSO + TEACl$ electrolyte.

Comparison between previous studies and the cycling performance obtained in this work is not easy and straightforward. For example, Cao et al.[30] used a trimethylammonium salt as additive in a highly concentrated zinc triflouromethanesulfonate ($Zn(OTf)_2$) water-in-salt electrolyte. This type of formulation reduces significantly the water activity, increasing not only Zn cycle life, but also, the stability potential window of aqueous electrolytes. However, this Zn^{2+} salt is 34 times more expensive than $ZnSO_4$, so this could be a reason to use the sulphate salt instead. On the other hand, Bayaguud et. Al[28] achieved great cycling stability by combination of QAC and a 3D copper current collector, thus the improved performance cannot be attributed solely to the additive but to a synergy between both factors. B. Bozzini et al.[29] reported relatively poor cyclability (below 100 h) at low current densities and areal capacities (1 mA cm^2 and 0.5 mAh cm^2) after addition of several QACs to a 2 M $ZnSO_4$ electrolyte. These authors also provided a detailed explanation, based on the Zn deposition morphology, of the positive effect that higher current densities can have on the cyclability of Zn//Zn symmetric cells previously observed by Glatz et al. .[58] This also puts in evidence the need for standardization of this test for electrolyte formulations since both current density and capacity can affect the stability of the Zn anode. Qiu et al.[59] also studied the effect of different QACs in a 2 M $ZnSO_4$, reaching a cycling time of 3000 h with addition of just 10 mM of TEABr. This surprisingly better performance could be the result of different cycling conditions (1 mA cm^{-2} and 1 mAh cm^{-2}) and a beneficial impact of relatively low concentrations of QACs (shown in the supplementary information of this manuscript, though no explanation is provided). Finally, it is worth mentioning that Cao et al.[26] also reached higher cycling times in a $ZnCl_2 - H_2O - DMSO$ (20 wt%). The effect of the anion on Zn cycling stability has been previously investigated by Wu et al.,[60] showing that Cl^- provides a better cyclability than SO_4^{2-} ion. Nevertheless, in chloride-based electrolytes, Cl_2 could be generated at high voltages in the cathode limiting the potential enhancement that could be obtained by addition of DMSO. Based on this, even though the performance obtained in

the 2 M $ZnSO_4$ containing DMSO and TEACl is not the best at the moment, the results proved that combining these two types of additives can lead to improvement in the cyclability of Zn anodes. Moreover, addition of TEACl decreases the overpotential when of the DMSO containing electrolyte. Thus, by optimizing the concentration of both compounds or testing other QAC, it might be possible to further improve the cycling stability of Zn anodes using this approach. Future efforts will be devoted to achieving this.

To test the electrolyte formulations in a full-cell configuration, AC//Zn hybrid supercapacitors devices were assembled and tested. Moreover, three-electrode CVs were recorded to determine the effect of DMSO and TEACl on the electrochemical response of AC electrodes (Fig 6-a). The results indicate that these additives have little effect on the capacitive behavior of the AC electrodes under study. The only noteworthy feature is the small peak on the anodic scan that appears in the TEACl containing electrolyte and could be due to the specific adsorption of Cl^- ions on the positively charged carbon electrode. This translates into a somewhat higher capacity as seen in Figure 6-b, reaching an initial value of 42 mAh g^{-}. In the other electrolytes, the capacity is not affected considerably by the changes in electrolyte composition (31–35 mAh g^{-}), though slightly higher initial values are recorded when both TEACl and DMSO are present. The capacity values are in the range of previously reported Zn-hybrid devices using AC as positive electrode,[61] with a charge-discharge behavior largely dominated by the capacitive electrode (Figure 6-c). In contrast, a clear improvement in cycling stability can be obtained after the addition of DMSO and TEACl, individually or combined. The cell assembled with just 2 M $ZnSO_4$ started showing signs of degradation after 1500 cycles, failing completely at 1700. Post-mortem SEM (Figs. 6-d and 6-e) shows the presence of a localized large cluster of Zn that seems to have penetrated the separator, suggesting that a short circuit of the cell was the reason for the failure. Figure 6-e shows the hexagonal Zn crystals aligned perpendicular to the electrode surface, in agreement with the results obtained from deposition experiments. XRD analysis of the electrodes of the four cells after cycling did not show the presence of other phases apart from Zn and hydrated $ZnSO_4$ probably arising from the electrolyte. As regards capacity retention, DMSO alone provides the best results with a value of 89% (considering the maximum capacity attained after the first cycles). In the case of TEACl and DMSO + TEACl, the retention is close to 85% and 62%, respectively. While a mechanistic study of the interaction between additives and the positive electrode is out of the scope of this work, these results remark the importance of optimizing the electrolyte formulation considering its final application. Therefore, for a set of additives, the best one in terms of Zn stability might not bring about the best improvements in terms of device performance.

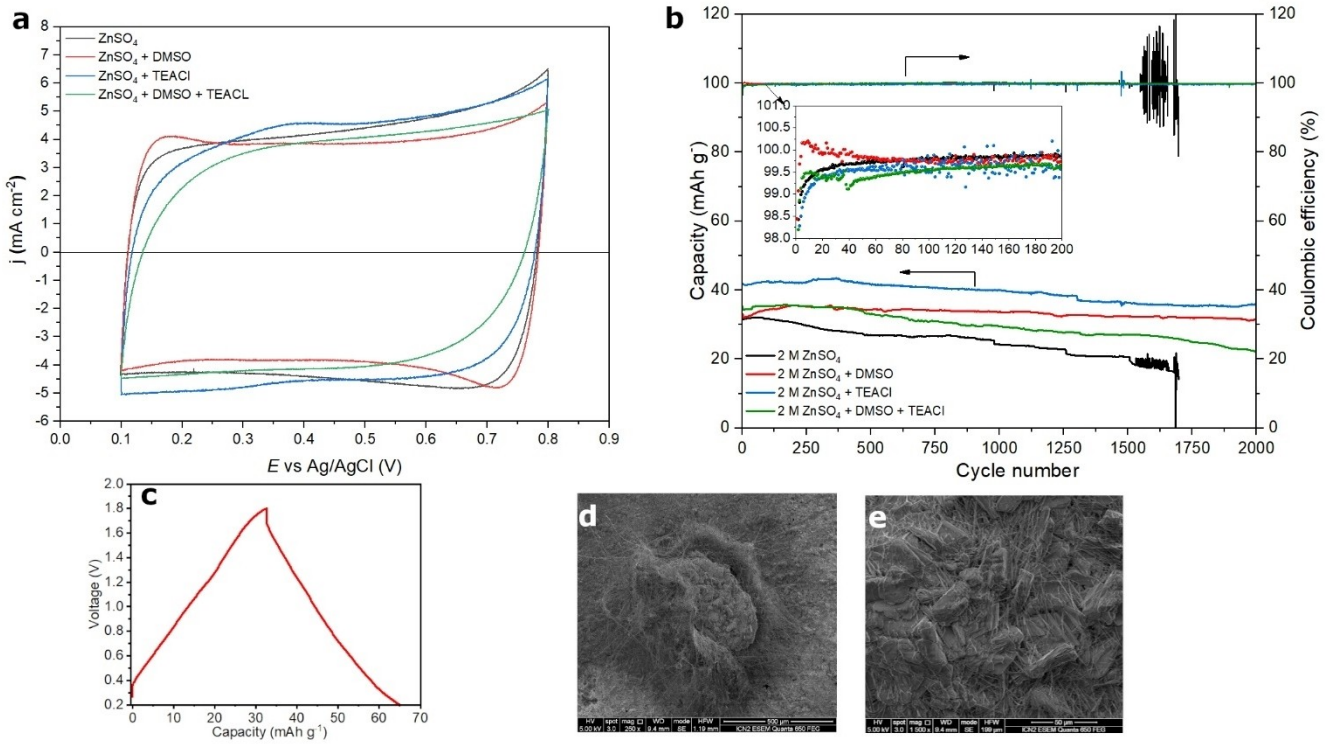

Figure 6. (a) CV of AC electrodes at 50 mV s^{-}. (b) Specific capacity and coulombic efficiency of Zn//AC hybrid supercapacitors (c) Typical galvanostatic charge-discharge profile of the Zn//AC devices, showing a clear capacitive behavior. SEM images of Zn anode after failure of the cell with 2 M $ZnSO_4$ electrolyte at (d) 250 X and (e) 1500X magnification.

Conclusions

The present work makes evident the advantages of performing simple and fast three-electrode measurements when assessing the potential of different additives for the formulation of more efficient electrolytes for Zn energy storage devices. This approach has been extensively used in the field of electroplating, which has led to a clear understanding and classification of additives and their action mechanism. The use of this configuration, gives information about the Zn electrode electrochemistry allowing for a proper characterization, avoiding the unwanted limitations that counter electrode may cause in commonly used coin-cells setups. The results reported in this study also show that combination of a complexing agent, DMSO, and a leveling one, like TEACl, can bring about great improvements in the cycle life and stability of Zn anodes. Once again, these formulations have proved to be successful in producing smooth and homogenous deposits in the plating industry. It is clear that the battery sector can greatly benefit from the knowledge gathered for more than a century. Furthermore, determination of kinetic parameters and evaluation of morphological and microstructural changes caused by different components of the electrolyte could also help predict the effect of these on the final performance of Zn anodes, especially detect the possibility of dendritic growth, main cause of short-circuit in Zn-based devices.

Although this approach is well-known, the only report on additives for Zn devices using it is that by Bozzini et al. Most articles just focus on the use of time-consuming cycling experiments without performing traditional electrochemical and deposition experiments. While at the time, both are still necessary, creating a database where a clear correlation between kinetic parameters, morphology changes and Zn cycling stability is established, might allow researchers to do a first screen of additives before doing long cycling tests in the future. Moreover, taking advantages of machine learning it may be possible to predict cycle life by just feeding the CV of a certain additive. Therefore, we hope this manuscript will serve as a starting point to encourage the battery community to employ this methodology to accelerate the development of more efficient energy storage devices.

Acknowledgements

The authors would like to acknowledge the financial support provided by Ministerio de Ciencia y Innovacion (MCIIN), the Agencia Estatal de Investigacion (AEI) and NextGenerationEU (TED2021-130205B-C2) for this research activity. L.N. Bengoa wants to thank the European Union for providing a Marie Curie Postdoctoral Fellowship (Grant 101062498-POMZAB) to join ICN2. The ICN2 is funded by the CERCA programme/Generalitat de Catalunya and supported by the Severo Ochoa Centres of Excellence programme, Grant CEX2021-001214-S, funded by MCIN/AEI/10.13039.501100011033.

Conflict of Interests

The authors declare no conflict of interest.

Data Availability Statement

The data that support the findings of this study are available from the corresponding author upon reasonable request.

Keywords: zinc · energy storage · hybrid devices · electrolyte additives · near-neutral

[1] J. Fu, Z. P. Cano, M. G. Park, A. Yu, M. Fowler, Z. Chen, *Adv. Mater.* **2017**, *29*, 1604685.
[2] M. Armand, J.-M. Tarascon, *Nature* **2008**, *451*, 652–657.
[3] A. R. Mainar, E. Iruin, L. C. Colmenares, A. Kvasha, I. De Meatza, M. Bengoechea, O. Leonet, I. Boyano, Z. Zhang, J. A. Blazquez, *J. Energy Storage* **2018**, *15*, 304–328.
[4] J. Zhang, Q. Zhou, Y. Tang, L. Zhang, Y. Li, *Chem. Sci.* **2019**, *10*, 8924–8929.
[5] D. Yang, H. Tan, X. Rui, Y. Yu, *Electrochem. Energy Rev.* **2019**, *2*, 395–427.
[6] M. M. Titirici, *Adv. Energy Mater.* **2021**, 2003700.
[7] D. Chao, W. Zhou, F. Xie, C. Ye, H. Li, M. Jaroniec, S.-Z. Qiao, *Sci. Adv.* **2020**, *6*, DOI 10.1126/sciadv.aba4098.
[8] J. Liu, C. Xu, Z. Chen, S. Ni, Z. X. Shen, *Green Energy & Environ.* **2018**, *3*, 20–41.
[9] G. Fang, J. Zhou, A. Pan, S. Liang, *ACS Energy Lett.* **2018**, *3*, 2480–2501.
[10] P. Gu, M. Zheng, Q. Zhao, X. Xiao, H. Xue, H. Pang, *J. Mater. Chem. A.* **2017**, *5*, 7651–7666.
[11] Y. Zeng, X. F. Lu, S. L. Zhang, D. Luan, S. Li, X. W. Lou, *Angew. Chem. Int. Ed.* **2021**, *60*, 22189–22194.
[12] B. Huang, J. Song, H. Kimura, Y. Li, Y. Xu, K. Yang, M. Cui, L. Du, L. Kang, *J. Power Sources* **2023**, *570*, 233048.
[13] Y. Li, H. Dai, *Chem. Soc. Rev.* **2014**, *43*, 5257–5275.
[14] J. Fu, R. Liang, G. Liu, A. Yu, Z. Bai, L. Yang, Z. Chen, *Adv. Mater.* **2019**, *31*, 1–13.
[15] X. Gong, J. Chen, P. S. Lee, *Batteries & Supercaps* **2021**, *4*, 1529–1546.
[16] N. R. Chodankar, S. J. Patil, S. Lee, J. Lee, S.-K. Hwang, P. A. Shinde, I. V. Bagal, S. V. Karekar, G. Seeta Rama Raju, K. Shanmugam Ranjith, D. P. Dubal, Y.-S. Huh, Y.-K. Han, C. R. Nilesh Chodankar, Y. Suk Huh, *InfoMat* **2022**, e12344.
[17] H. Wang, W. Ye, Y. Yang, Y. Zhong, Y. Hu, *Nano Energy* **2021**, *85*, 105942.
[18] A. R. Mainar, L. C. Colmenares, J. A. Blázquez, I. Urdampilleta, *Int. J. Energy Res.* **2018**, *42*, 903–918.
[19] J. Yang, B. Yin, Y. Sun, H. Pan, W. Sun, B. Jia, S. Zhang, T. Ma, *Nano-Micro Lett.* **2022**, *14*, DOI 10.1007/s40820-021-00782-5.
[20] G. D. D. Wilcox, P. J. J. Mitchell, *J. Power Sources* **1989**, *28*, 345–359.
[21] Z. Zhan, *Int. J. Electrochem. Sci.* **2021**, *16*, 210334.
[22] J.-C. Hsieh, C.-C. Hu, T.-C. Lee, *J. Electrochem. Soc.* **2008**, *155*, D675.
[23] S. Guo, L. Qin, T. Zhang, M. Zhou, J. Zhou, G. Fang, S. Liang, *Energy Storage Mater.* **2021**, *34*, 545–562.
[24] Z. Liu, J. Ma, X. Liu, H. Wu, D. Wu, B. Chen, P. Huang, Y. Huang, L. Wang, Z. Li, S. Chou, *Chem. Sci.* **2022**, *14*, 2114–2122.
[25] S. Hosseini, A. Abbasi, L. O. Uginet, N. Haustraete, S. Praserthdam, T. Yonezawa, S. Kheawhom, *Sci. Rep.* **2019**, *9*, DOI 10.1038/s41598-019-51412-5.
[26] L. Cao, D. Li, E. Hu, J. Xu, T. Deng, L. Ma, Y. Wang, X.-Q. Q. Yang, C. Wang, *J. Am. Chem. Soc.* **2020**, *142*, 21404–21409.
[27] D. Feng, F. Cao, L. Hou, T. Li, Y. Jiao, P. Wu, *Small* **2021**, *17*, DOI 10.1002/smll.202103195.
[28] A. Bayaguud, X. Luo, Y. Fu, C. Zhu, *ACS Energy Lett.* **2020**, *5*, 3012–3020.
[29] B. Bozzini, M. Boniardi, T. Caielli, A. Casaroli, E. Emanuele, L. Mancini, N. Sodini, J. Strada, *ChemElectroChem* **2023**, *202201130*, DOI 10.1002/celc.202201130.
[30] L. Cao, D. Li, T. Pollard, T. Deng, B. Zhang, C. Yang, L. Chen, J. Vatamanu, E. Hu, M. J. Hourwitz, L. Ma, M. Ding, Q. Li, S. Hou, K. Gaskell, J. T. Fourkas, X. Q. Yang, K. Xu, O. Borodin, C. Wang, *Nat. Nanotechnol.* **2021**, *16*, 902–910.
[31] J.-C. Hsieh, C.-C. Hu, T.-C. Lee, *Surf. Coat. Technol.* **2009**, *203*, 3111–3115.

[32] J. L. Ortiz-Aparicio, Y. Meas, G. Trejo, R. Ortega, T. W. Chapman, E. Chainet, *J. Appl. Electrochem.* **2013**, *43*, 289–300.
[33] J. L. Ortiz-Aparicio, Y. Meas, T. W. Chapman, G. Trejo, R. Ortega, E. Chainet, *J. Appl. Electrochem.* **2015**, *45*, 67–78.
[34] J. F. Parker, J. S. Ko, D. R. Rolison, J. W. Long, *Joule* **2018**, *2*, 2519–2527.
[35] A. M. Alfantazi, D. B. Dreisinger, *J. Appl. Electrochem.* **2001**, *31*, 641–646.
[36] I. Zouari, F. Lapicque, *Electrochim. Acta* **1992**, *37*, 439–446.
[37] M. C. H. McKubre, *J. Electrochem. Soc.* **1981**, *128*, 524.
[38] M. Cai, *J. Electrochem. Soc.* **1996**, *143*, 2125.
[39] W. Kao-ian, M. T. Nguyen, T. Yonezawa, R. Pornprasertsuk, J. Qin, S. Siwamogsatham, S. Kheawhom, *Mater. Today Energy* **2021**, *21*, 100738.
[40] J. C. Ballesteros, E. Chaînet, P. Ozil, G. Trejo, Y. Meas, *Electrochim. Acta* **2011**, *56*, 5443–5451.
[41] J. O. Bockris, Z. Nagy, A. Damjanovic, *J. Electrochem. Soc.* **1972**, *119*, 285.
[42] A. R. Despić, D. Jovanović, T. Rakić, *Electrochim. Acta* **1976**, *21*, 63–77.
[43] J.-R. Park, H.-T. Kim, *Plating & Surface Finishing*, **1999**.
[44] S. Fletcher, *J. Solid State Electrochem.* **2009**, *13*, 537–549.
[45] A. J. Bard, L. R. Faulkner, in *Electrochemical Methods. Fundamental and Applications*, John Wiley & Sons, Inc., New York, **2001**, pp. 87–136.
[46] R. Winand, *Hydrometallurgy* **1992**, *29*, 567–598.
[47] K. I. Popov, N. D. Nikolic, in *Electrochemical Production of Metal Powders* (Ed.: S. S. Djokić), Springer Science + Business Media, New York, **2012**, pp. 1–62.
[48] N. D. Nikolić, P. M. Živković, J. D. Lović, G. Branković, *J. Electroanal. Chem.* **2017**, *785*, 65–74.
[49] L. N. Bengoa, S. Bruno, H. A. Lazzarino, P. R. Seré, W. A. Egli, *J. Appl. Electrochem.* **2014**, *44*, 1261–1269.
[50] M. Paunovic, M. Schlesinger, in *Fundamentals of Electrochemical Deposition*, John Wiley & Sons, Inc., **2006**, pp. 177–198.
[51] H. Park, J. A. Szpunar, *Corros. Sci.* **1998**, *40*, 525–545.
[52] J. C. Ballesteros, C. Gómez-Solís, L. M. Torres-Martínez, I. Juárez-Ramírez, *Int. J. Electrochem. Sci.* **2015**, *6*, 1597–1616.
[53] R. Juškenas, V. Pakštas, A. Sudavičius, V. Kapočius, V. Karpavičiene, *Appl. Surf. Sci.* **2004**, *229*, 402–408.
[54] L. Ma, M. A. Schroeder, O. Borodin, T. P. Pollard, M. S. Ding, C. Wang, K. Xu, *Nat. Energy* **2020**, *5*, 743–749.
[55] L. H. Mendoza-Huizar, J. Robles, M. Palomar-Pardavé, *J. Electroanal. Chem.* **2002**, *521*, 95–106.
[56] I. H. Omar, H. J. Pauling, K. Juettner, *J. Electrochem. Soc.* **1993**, *140*, 2187–2192.
[57] M. Tribbia, J. Glenneberg, G. Zampardi, F. La Mantia, *Batteries & Supercaps* **2022**, *5*, DOI 10.1002/batt.202100381.
[58] H. Glatz, E. Tervoort, D. Kundu, *ACS Appl. Mater. Interfaces* **2020**, *12*, 3522–3530.
[59] Q. Qiu, X. Chi, J. Huang, Y. Du, Y. Liu, *ChemElectroChem* **2021**, *8*, 858–865.
[60] S. Wu, Y. Chen, T. Jiao, J. Zhou, J. Cheng, B. Liu, S. Yang, K. Zhang, W. Zhang, *Adv. Energy Mater.* **2019**, *9*, DOI 10.1002/aenm.201902915.
[61] L. Dong, X. Ma, Y. Li, L. Zhao, W. Liu, J. Cheng, C. Xu, B. Li, Q. H. Yang, F. Kang, *Energy Storage Mater.* **2018**, *13*, 96–102.

Manuscript received: October 9, 2023
Revised manuscript received: November 30, 2023
Version of record online: February 22, 2024